Rapid Composite Tube Manufacture Utilizing the QuickstepTM Process

Michael D. Silcock, Claudia Garschke, Wayne Hall and Bronwyn L. Fox

The online version of this article can be found at:

http://jcm.sagepub.com/content/41/8/965

Published by:

$SAGE

http://www.sagepublications.com

On behalf of:

American Society for Composites

Additional services and information for *Journal of Composite Materials* can be found at:

Email Alerts: http://jcm.sagepub.com/cgi/alerts

Subscriptions: http://jcm.sagepub.com/subscriptions

Reprints: http://www.sagepub.com/journalsReprints.nav

Permissions: http://www.sagepub.com/journalsPermissions.nav

Citations: http://jcm.sagepub.com/content/41/8/965.refs.html

>> Version of Record - Jul 5, 2007

What is This?

Rapid Composite Tube Manufacture Utilizing the Quickstep™ Process

MICHAEL D. SILCOCK*, CLAUDIA GARSCHKE, WAYNE HALL
AND BRONWYN L. FOX
*Centre for Material and Fiber Innovation, Deakin University
Geelong, 3217, Australia*

ABSTRACT: In this study, a novel method for manufacturing composite tubes utilizing the Quickstep™ process has been developed. Tubes manufactured from 'quick-cure' Toray G83C prepreg have demonstrated highly repeatable axial crush behavior with an average specific energy absorption (SEA) of 86 kJ/kg. The cure cycle is optimized by comparing the results from compression, dynamic mechanical thermal analysis (DMTA), differential scanning calorimetry (DSC), and porosity testing. The tube lay-up is optimized using compression and porosity test results. The effect of changes in fiber-orientation on SEA is also investigated. Process development has resulted in a robust manufacturing method capable of producing fully cured, high performance composite tubes with a cure cycle of 7 min. This corresponds to a 95% reduction in time compared to an equivalent autoclave cycle.

KEY WORDS: compression, dynamic mechanical thermal analysis (DMTA), differential scanning calorimetry (DSC), manufacture, crashworthiness, composite, tubes, axial crushing, specific energy absorption, glass transition temperature.

INTRODUCTION

VEHICLE SAFETY IS of considerable interest to both the public and auto-manufacturers, hence numerous studies in this field have been undertaken and reported [1–4]. The conflicting requirements for manufacturers to improve vehicle crashworthiness and reduce vehicle weight and emissions, yet provide features such as air conditioning and power steering have forced the manufacturers to investigate lighter and less conventional materials. Composites are capable of simultaneously providing both reduced weight and improved crashworthiness through higher levels of energy absorption and improved energy absorption mechanisms [5]. Subsequently, these materials have been the focus

---

of a number of investigations in recent years [6–11]. Such related work focussed on characterizing the influence of various parameters on the crush mode and energy absorption but no reports have linked a production technique to these attributes.

Though the benefits of using such materials have been outlined repeatedly, they have only been employed in low-volume prestige vehicles and several classes of racing, particularly Formula 1, primarily due to the expensive raw material and high manufacturing and processing costs [12]. These costs inhibit most automotive manufacturers from prototyping or implementing designs without significant outlay. To further compound the issue, no analytical or numerical tools currently exist which can predict the stiffness, strength, and post-failure behavior of a composite structure of a general shape [7]. As a result, composites have not yet been fully utilized in automotive applications.

For composites to be employed in widespread automotive applications, significantly shorter processing times and lower capital and tooling costs are essential. The Quickstep^{TM} process (www.Quickstep.com.au) is an advanced composite manufacturing process for out-of-autoclave processing of high quality, low cost, lightweight components using faster cure cycles. This process utilizes a unique fluid filled mold to provide exceptional heat transfer, temperature control, and reduced cure times. These attributes together with significantly lower capital, tooling, and operational expenses make Quickstep an attractive process [13]. Work by Zhang and Fox [14] has shown that the Quickstep^{TM} process can improve the Mode I fracture toughness of composites. This property contributes to the energy absorption of composite tubes. As the focus of the underlying study is crashworthiness, or more specifically understanding the fundamental behavior of composite tubes under axial load, the development of a tool specifically for the manufacture of these structures was a natural progression. Current methods of tube manufacture include pultrusion, filament winding, and autoclave mandrel wrapping.

EXPERIMENTAL

Materials

Toray G83C epoxy prepreg was obtained from Toray Composites (America). The matrix used in this prepreg has been specifically formulated for reduced cure cycle times [15]. Three types of fiber reinforcements were used, 5-harness satin weave, designated T700S 12K 5HS/G83C (370 gsm and 40% resin content) for general testing, and 2×2 twill, designated T700S 12K 2×2 Twill/G83C (370 gsm and 40% resin content), and unidirectional material, designated T600S/G83C (190 gsm and 38% resin content) for the work investigating the influence of fiber orientation on specific energy absorption (SEA). The G83C prepreg was selected as it is available in several forms, all of which utilize the same resin and similar fiber properties. Throughout this work, a 0° fiber-orientation refers to fibers laid along the length of the tubes and a 90° orientation follows the circumference.

Process

A prototype mandrel was constructed from 6061-T6 aluminum. The design utilizes a 1200 mm long, 60 mm OD circular tube section, capped at one end, with a 10 mm thick
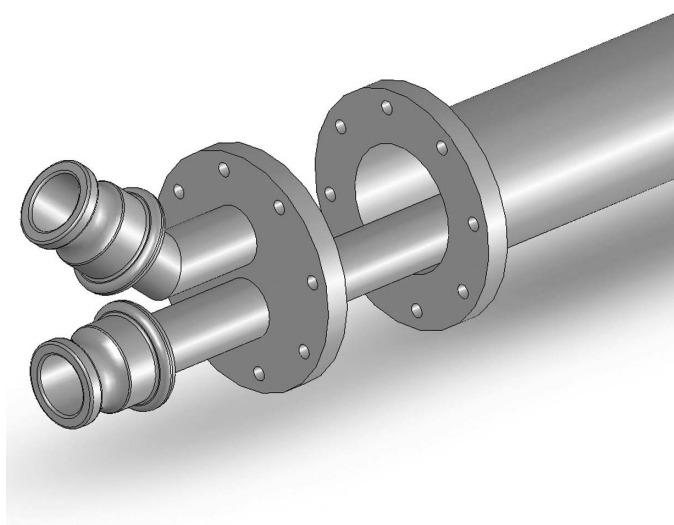
Figure 1. *CAD image of mandrel showing quick-release cam-locks and fluid inlet (lower) and outlet (upper).*

flange with eight M6 bolts, at the other. The capped end employs an aluminum plate insert, which was welded in place before being machined to ensure a smooth outer surface. Mating to the flange is a 10 mm thick plate, which holds the Quickstep inlet/outlet connections as shown in Figure 1. The inlet pipe extends 1100 mm through the inside of the mandrel, unlike the outlet, which extends only to the reverse side of the flange at the connection point. The ends of the connectors utilize cam-lock, quick-release hose connectors allowing the mandrel to be disconnected and moved easily. Though the prototype is circular, it is expected that any near-symmetrical cross-section can be used.

Prior to each wrapping process, the surface of the mandrel was cleaned and then treated with a releasing agent (Frekote 44-NC), to ensure that no surface contaminants were present. A section of the preimpregnated carbon fiber was then cut and rolled onto the mandrel by hand with care taken to avoid entrapping air between the layers. This was facilitated by the use of a heat-gun on the material as it was applied which ensured a high degree of tack. This method of application produced a 4-layer 'swiss roll' type lay-up as can be seen in Figure 2. Thermocouples were inserted between the material and the mandrel at each end for monitoring component temperatures during the cure. One of several lay-up configurations (described shortly) were then applied and the tubes were left under vacuum (where possible) to debulk for at least 30 min prior to curing. The temperature and flow rate of the fluid in the Quickstep was controlled manually.

During the lay-up process, application of both the perforated release film ('WL5200' produced by Airtech) and breather bag involved wrapping a single layer over the composite tube's surface. Two thicknesses of breather bag were used, the thicker was 'airweave N10' produced by Airtech, the thinner was 'Airbleed 120' from Aerovac. Airtech's shrink tape product 'Wrightlon 4500' was used which specifies a 5% shrink at 176°C. Shrink tape application was achieved with the use of a lathe with the mandrel's connector end supported by a nylon ring inside the lathe's steady with the capped end held

Figure 2. Schematic of typical 'swiss roll' lay-up produced when prepreg is wrapped onto mandrel.

inside a three-jaw self-centring chuck. Shrink tape rolls were held in a four-way tool-post and the required overlap of 3–4 mm was achieved using the auto-feed. The shrink tape rolls were pressed between two plates, forced together with springs by which, altering the compression on the springs (hence plates) would alter the tension of the shrink tape being applied. Vacuum bag application involved sealing a rectangular shaped bag across the top of the mandrel (between the Quickstep connector flange and composite tube) and extending approximately 300 mm past the end of the tube for inclusion of a vacuum port. 'Wrightlon 7400' obtained from Airtech, was used.

During the cure cycle, temperatures of up to 155°C were used, causing the aluminum to expand, applying pressure to the tube internally. Once the epoxy was cured, the mandrel was flushed with ambient temperature fluid, allowing the aluminum to shrink back to its original size. The difference in thermal expansion coefficients of the two materials facilitates the removal of the cured tube. This produced tubes of ~1000 mm in length. The ends of the tubes were removed prior to cutting the remainder into nine or ten samples. These smaller samples were of 100 mm length, 60 mm ID, ~2 mm thick, and weighed 50–55 g.

The manufacturer-recommended autoclave cure cycle for Toray G83C [15] suggests a dwell at 150°C for 5–10 min, followed by cooling to 45°C. Assuming a 2.5°C/min ramp-rate, the resulting cure cycle time is 130 min [13]. Based on the manufacturer's recommendations [15], a standard Quickstep cure cycle was established which consisted of a 5 min dwell at 100°C followed by a 3 min dwell at 150°C before being cooled to less than 45°C, shown schematically in Figure 3. This cure cycle was optimized as described in the cure cycle optimization section of this article. This cure cycle takes a total of 14 min – an 88% reduction in time over the autoclave process. A benefit of using the aforementioned aluminum mandrel was its low latent heat and high thermal conductivity, which resulted in remarkable ramp rates (average 40°C/min on ramp-up for the 14 min cure cycle and 70°C/min during ramp-down for all cycles).

Test Specifications

In order to establish the effect of the cure cycle, lay-up configuration, and fiber orientations, several tests were conducted. Compression testing of the tubes was
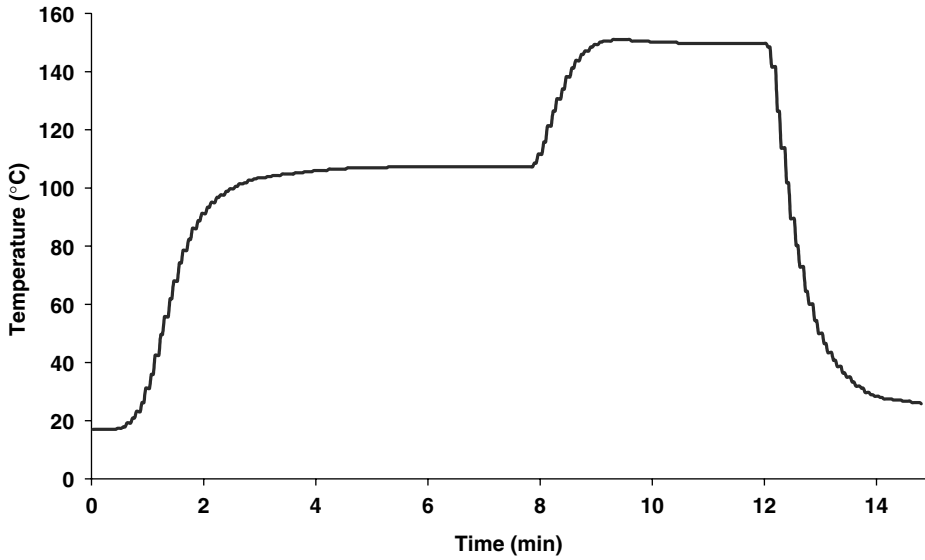
Figure 3. *Actual cure profile for 14 min cure showing the ramp-rate.*

performed in an MTS testing machine between two flat platens at 10 mm/min. Each tube manufactured was approximately 1 m in length allowing for at least nine samples for compression testing, however, typically five samples from various positions on the mandrel were tested. Some compression testing of the first several tubes has been carried out and reported in a previous paper [16]. Tubes TSP-1, 2, 3, and 4 were crushed in a hydraulically driven 385 kN MTS with Teststar 2s control software utilizing a 385 kN MTS load cell. All following tubes were crushed in a screw-driven 100 kN MTS 20/G with Testworks 4 (V.4.01) control software with a 100 kN MTS load cell. The change in MTS was deemed necessary due to the accurate range of the 385 kN being >50 kN in compression (average loads of 45–55 kN were observed). A control test was performed to ensure the calibration of both the machines. A sequence of a compression test is shown in Figure 4.

Prior to compression testing, each tube had a 45° chamfer turned into one of the ends which ensures that a progressive failure mode is produced [5]. Each tube was then weighed and all tubes were crushed with the load-displacement data recorded. The energy absorbed was calculated by integrating the load and displacement as shown in Equation (1) [17].

$$E_a = \int P \mathrm{d}l \quad [\mathrm{kJ}] \tag{1}$$

where P = load (N) and l = crush length (m).

The SEA is the energy absorbed per unit mass and was calculated by dividing the energy absorbed by the mass of the crushed tube, as shown in Equation (2).

$$\mathrm{SEA} = \frac{E_a}{m_{\mathrm{crushed}}} \left[\frac{\mathrm{kJ}}{\mathrm{kg}} \right]. \tag{2}$$
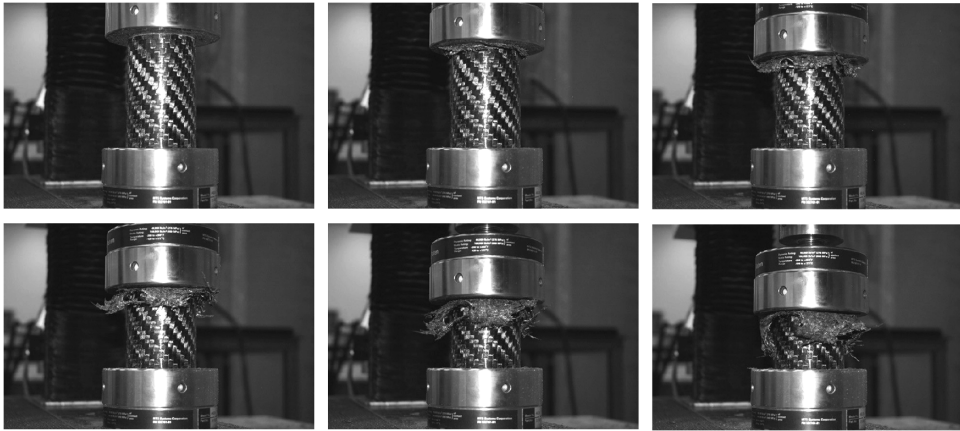
Figure 4. *Compression testing sequence of TFO-2.*

Figure 5. *An example of the splaying mode of progressive failure observed in compression testing of TFO-0.*

As expected, all crushed tubes failed progressively, most of them in the splaying mode [18], an example of which can be seen in Figure 5.

Early developmental work raised concerns about a potential temperature difference along the length of the 1 m long tube and the effect of temperature gradients on the energy of absorption. To determine whether this adversely affected the energy absorption, the third tube manufactured was cut into 10 separate samples and these were crushed with excellent reproducibility. Therefore, the lengthwise location of the tube sample prior to testing was shown to be inconsequential.

Dynamic mechanical thermal analysis (DMTA) was conducted on a Rheometrics Scientific IV. The instrument was computer controlled and the proprietary software used is known as 'Orchestrator'. All samples were run on a large frame in dual cantilever mode. A multifrequency analysis was undertaken at 1, 10, 50, and 100 Hz, over a temperature range of 25–250°C, at a heating rate of 5°C/min. Glass transition temperatures were derived by the $\tan \delta$ peak position at 1 Hz.

Differential scanning calorimetry (DSC) analyses were conducted on a Mettler Toledo 821 with 'Star Software' version 6. Samples were run at a heating rate of 10°C/min under nitrogen. A sample size of between 10 and 30 mg was used. The DSC was used to identify whether the samples had reached the highest attainable degree of cure.

For porosity testing, 10 samples were chosen as representative of each tube, 5 central specimens and 5 from an end. Samples were set in resin and polished to 1 μm. Images were taken by an Olympus BX51M microscope at a magnification of 100× and analyzed by OLYSIA m3 imaging software.

RESULTS

Cure Cycle Optimization

During cure cycle optimization, tubes were prepared with a perforated release film, N10 breather, and vacuum bag. All tubes experienced identical treatment and debulk times.

Four variations of the quickstep cure cycle were tested, these are shown schematically in Figure 6. One cycle held the part at full temperature for the minimum 3 min, excluding the intermediate dwell period used in the standard cure cycle. This resulted in a 7 min cure (cure cycle B), a 95% reduction in time over the autoclave cycle. The two longer cures, cycles C and D, tested the effectiveness of the dwell and full-temperature times of the standard, 14 min cure (cure cycle A). A post-cure was performed on four tubes manufactured by the 7 and 14 min cure cycles (two from each cycle). Tubes were post-cured for 2 h at 150°C in an oven.

Altering the cure cycle had very little effect on the appearance of the tubes, other than some light pitting evident on tubes cured in 7 min – a result of the 'snap cure', which did not have an intermediate dwell at 100°C. Further testing confirmed an increase in the
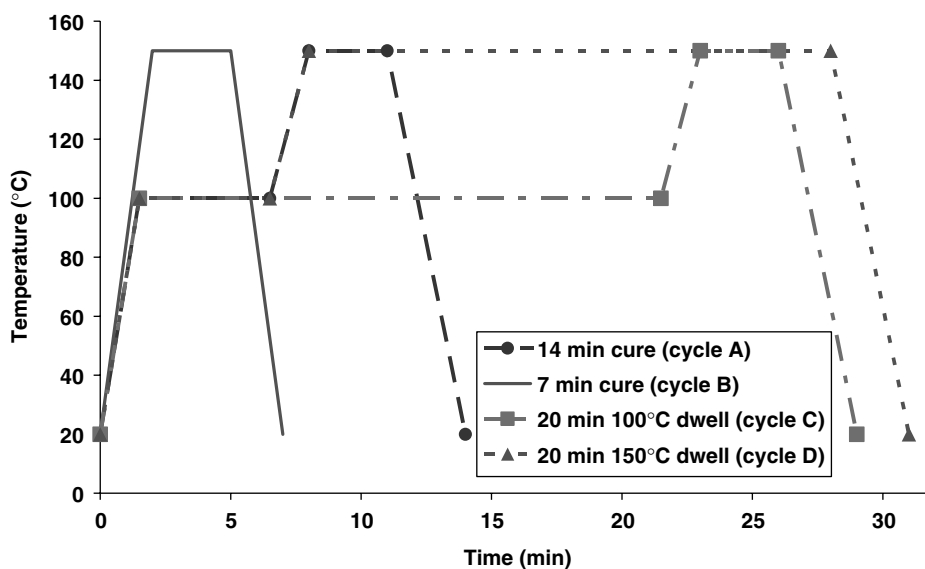
Figure 6. *Various cure cycles used in testing.*

(a)   (b)
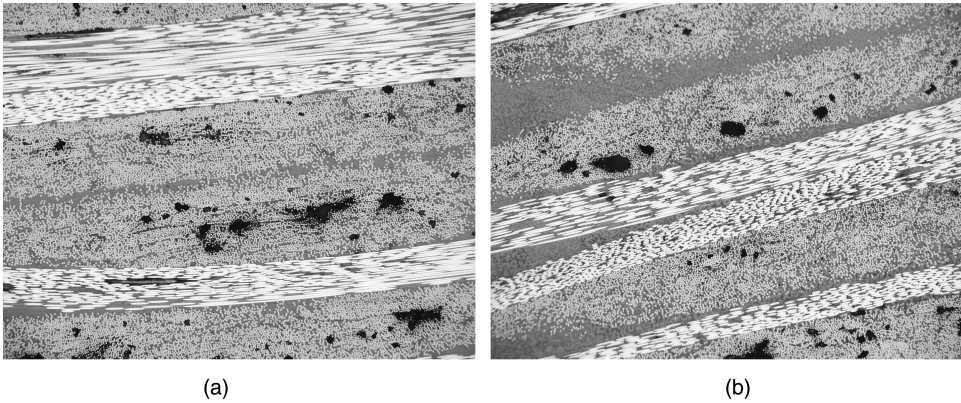
Figure 7. *Typical porosity images for (a) 7 and (b) 14 min cure cycles (100×).*
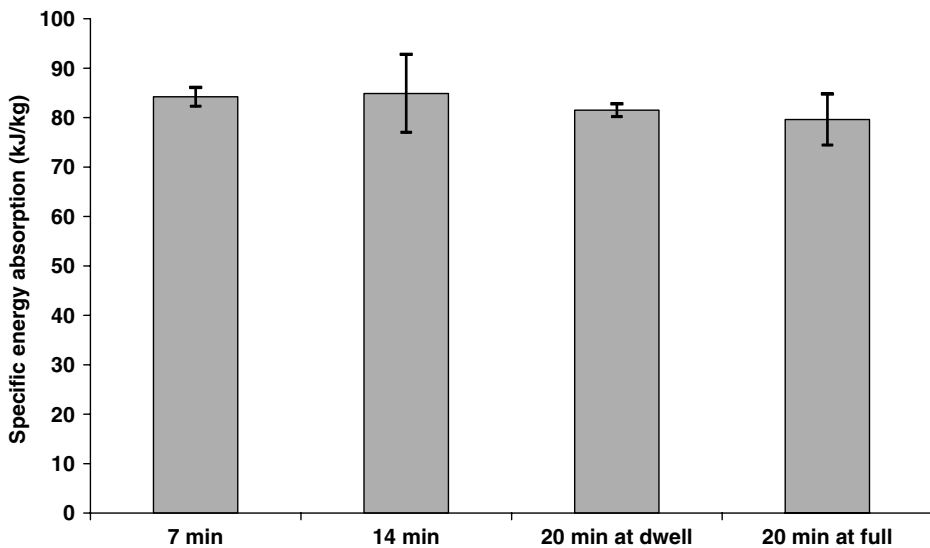
Figure 8. *SEA figures for various cure cycles (±2σ).*

porosity of the tubes manufactured by the 7 min cure (cure cycle B) compared with those from the 14 min cure (cure cycle A) with average void contents of 5.21 and 4.24%, respectively. Examples of typical optical microscope analysis specimens can be seen in Figure 7. In an attempt to reduce the tube porosity further, a 3-layer [0/90] tube was manufactured where each layer was debulked after being applied to the mandrel and cured with cycle A. The porosity values for this specimen averaged 6.05%. No improvements were observed with the longer cure cycles. Despite the varying porosity levels, the effect was not evident in compression testing as all cure cycles produced tubes of very similar SEA values, as shown in Figure 8.

While the energy absorption of the tubes is similar for all cure cycles, there is a noticeable trend in the glass transition temperatures as measured by DMTA. The average T_g for tubes cured with the 14 min cycle (cure cycle A) was 174°C whereas the average T_g
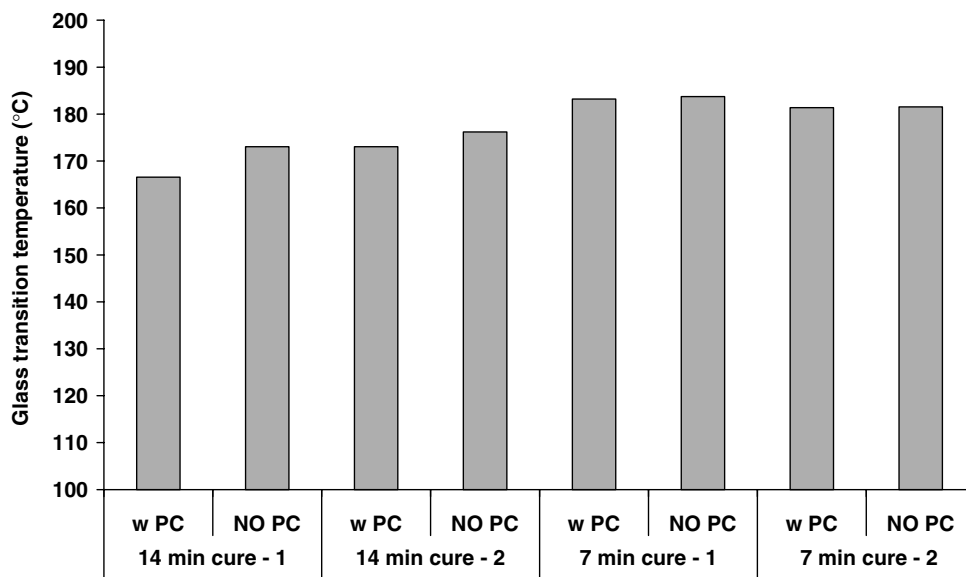
Figure 9. *Glass transition temperatures for 7 and 14 min cure cycles with post-cure (w PC) and without post-curing (NO PC). Values are obtained from tan δ peaks from DMTA.*

for tubes cured with the 7 min cycle (cure cycle B) was 183°C. The same trend may be observed even after the tubes have been post-cured, as can be seen in Figure 9. The authors attribute the increased T_g associated with the shorter cure cycle to be a result of the higher temperature ramp rates associated with this cycle, being 65°C/min compared with 40°C/min in cycle A. The effect of high temperature ramp rates during cure on the glass transition temperature of composites has also been observed in a study by Fang and Scola [19]. This comparison of thermal and microwave cure processes found that higher T_gs were observed in microwave cured composites, where the heating rate was much higher than in the autoclave cured composites. The T_gs in this reference were measured using tan δ peaks (at 1 and 10 Hz), with increases of up to 15°C observed when the composites were cured using microwaves. In the current study, a small reduction in T_g was observed for post-cured tubes from the 14 min cure cycle, although this was most likely caused by experimental error as the same trend was not apparent for the post-cured 7 min cure cycle tubes. Post-cured tubes demonstrated no variation in crush performance.

The DSC testing showed no difference between samples cured by cycles A or B, either with or without post-cure. Comparison of the enthalpy curves (for the T_g transition) showed only straight lines with no apparent peaks (making the calculation of the exact degree of cure extremely difficult), confirming that the highest possible degree of cure had been reached with the 7 min cycle.

Lay-up Optimization

Several lay-up configurations were tested in order to improve the manufacturability, performance and appearance of the tubes. The first five tubes were wrapped with a layer of perforated release film, N10 or N4 breather and a conventional vacuum bag.

Table 1. Variations of lay-up configuration.

	Plies	Lay-up	Cure time	Lay-up configuration	Surface finish/appearance
TSP-1	4	[0/90]	14 min	Perforated release film breather (N10) vacuum bag	Poor External-coarse and grainy, light axial ridges. Internal-light pitting.
TSP-2	4	[0/90]	14 min	Perforated release film breather (N4) vacuum bag	Poor External-little rough, light axial ridges. Internal-light pitting.
TSP-3	4	[0/90]	14 min	Shrink tape only	Acceptable External-smooth, noticeable pitting. Internal-light pitting.
TSP-4	4	[0/90]	14 min	Shrink tape breather (N10) vacuum bag	Excellent External-excellent, smooth. Internal-extremely light pitting.

This approach resulted in light axial ridges along the length of the tubes and a rough, grainy appearance, which was deemed unacceptable for production purposes and likely to affect the mechanical properties. Shrink tape was then employed to counteract this problem and provide consolidation pressure. Several tubes were then manufactured using only shrink tape but the surfaces (both inner and outer) of these tubes exhibited pitting, therefore, N10 breather and vacuum bags were applied over the shrink tape. This was adopted as the standard procedure. The various lay-up configurations can be seen in Table 1.

Tubes manufactured with the various lay-up configurations displayed very little difference in energy absorption despite several samples possessing flaws. During the manufacture of TSP-1 and TSP-2, axial ridges formed along their lengths. Interestingly, this had little effect on the crush performance of the tubes but initiated an investigation into shrink tape. An example of a shrink tape tube is shown in Figure 10. The introduction of shrink tape, as well as improving appearance, increased the energy absorption fractionally (as can be seen in Figure 11) and reduced sample porosity slightly.

Fiber Orientation Testing

To aid in the development of the process, a single length of woven prepreg was wrapped onto the mandrel, resulting in tubes with a 4-layer, [0/90] configuration without seams. Work by Farley [8] has shown that this is the least effective lay-up for energy absorption and significant improvements in SEA are possible with orientations of [0/±15]. The various orientations tested are shown in Table 2 including the specific form of the material used. It should be noted that all tests were performed using the various forms of Toray G83C and cured with cycle A.

No significant improvement in SEA was achieved by altering the fiber orientation as can be seen in Figure 12. TFO-1 was designed to investigate the effect of fiber discontinuities with 4 layers applied in separate pieces so that their seams were 90° apart. This would effectively isolate the influence of these seams, an important consideration as the following tubes were manufactured in separate pieces. Five samples were crushed which

Figure 10. *TSP-4 surface finish.*
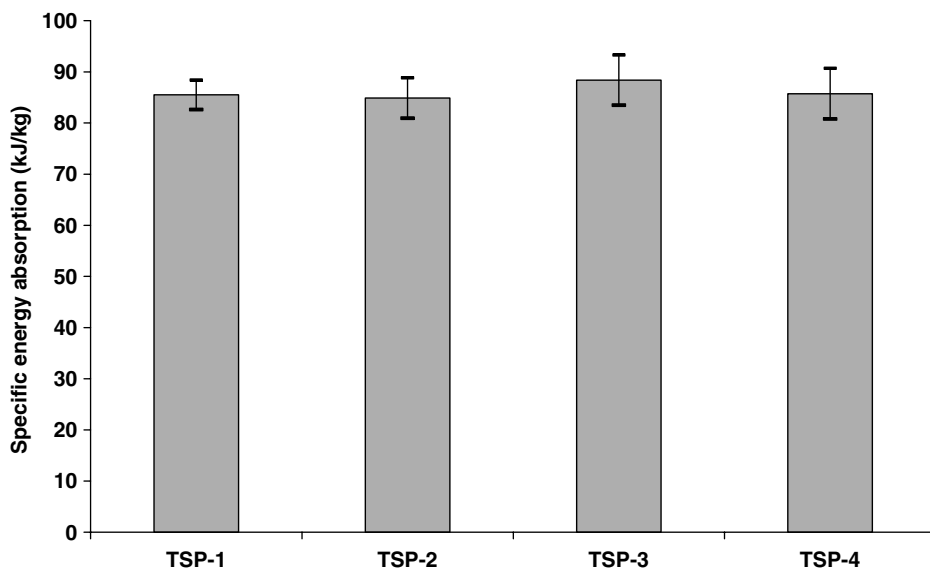
Figure 11. *Specific energy absorption figures for various lay-up configurations ($\pm 2\sigma$).*

demonstrated that this had little effect on the SEA figures and verified that further lay-ups would be unaffected by separating the layers. Notable reductions in SEA values were observed in tubes TFO-3 and TFO-4, whose purpose was to identify whether axial or hoop fibers contribute more to the energy absorption. As was demonstrated, hoop fibers (TFO-4) contribute the most, although an interaction between the hoop and axial fibers is required to produce much greater SEA values. The highest recorded SEA in all tests was 94.5 kJ/kg.

Table 2. Fiber orientations tested.

	Layers	Fiber orientation
TFO-0	4	$[0/90]_H$ (standard – 1 piece)
TFO-1	4	$[0/90]_H$ in 4 separate pieces
TFO-2	4	$[+15/-75,-15/+75]_{S\ T}$
TFO-3	4	$[\pm45,0,0,\pm45]_{T\ U}$
TFO-4	4	$[\pm45,90,90,\pm45]_{T\ U}$
TFO-5	3	$[0/90,\pm45,0/90]_T$

Subscripts 'S', 'H', 'T' and 'U' denote (S)ymmetric, (H)arness, (T)will and (U)nidirectional, respectively.
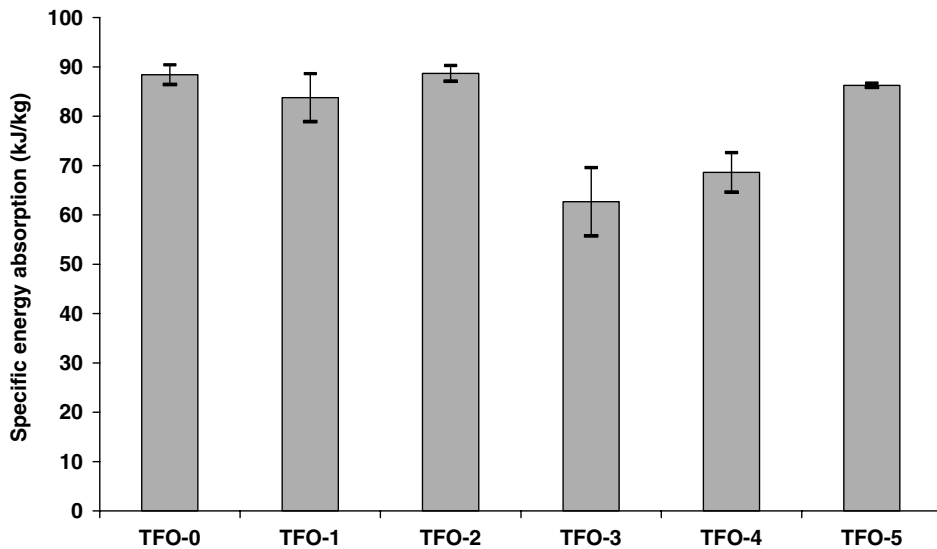
Figure 12. *Specific energy absorption figures for various fiber-orientations ($\pm2\sigma$).*

CONCLUSIONS

A novel technique for manufacturing composite tubes which takes advantage of the Quickstep's rapid cure cycles has been described and the effect of key processing parameters was investigated. Specifically, the effect of the cure cycle, lay-up configuration and composite fiber-orientation was tested by axial crush testing, DMTA, DSC, and porosity analysis.

A standard cure cycle of 14 min was employed and validated by testing several similar variations. One variation eliminated the dwell period, resulting in a 7 min cure cycle, 95% quicker than the autoclave cure. The DSC testing concluded that all cure cycles reached the highest attainable degree of cure while a marginal increase in porosity was observed for the 7 min cure cycle. The DMTA results indicate that the shorter 7 min cure achieves distinctly higher T_gs, potentially a result of the increased ramp-rate and exclusion of the intermediate dwell. Ramp-rates of up to $160°$C/min were observed in testing, 98% higher than those seen in autoclave processing. No improvement in SEA, T_g, porosity, or degree of cure was observed from extended periods at intermediate dwell or full temperature or when a post-cure was employed.

A conventional vacuum bag produced significant aesthetic imperfections in the form of axial ridges. The introduction of shrink tape eliminated this issue and produced smooth tubes with no apparent flaws. Despite the removal of these flaws from the process, only marginal improvements in SEA and porosity were observed.

A baseline average SEA figure of 86 kJ/kg was obtained for several tubes of 4-layer [0/±90] lay-ups in either 5-harness satin weave or 2 × 2 twill. Other materials commonly used in automotive crash applications are aluminum and steel whose typical SEA values are 20 and 30 kJ/kg respectively [20]. No further improvements were made by altering the orientation of the fibers. However, notable SEA reductions for tubes of [±45,0,0,±45] and [±45,90,90,±45] indicate that interactions between the hoop and axial fiber components are vital for higher degrees of energy absorption. In the lay-ups described, the hoop fibers were observed to contribute more than axial fibers. The highest SEA value produced in testing was 94.5 kJ/kg.

A rapid and robust composite tube manufacturing process has been developed which has shifted the rate-limiting step to the lay-up process. This process not only has the potential to unlock new markets and applications, but also to enable widespread use in markets where the benefits of such structures can now be obtained at a fraction of the time and cost.

REFERENCES

1. Botkin, M., Browne, A. and Johnson, N. (1998). Development of a Composite Front Structure for Automotive Crashworthiness, *ASME – Crashworthiness, Occupant Protection and Biomechanics in Transportation Systems*, Anaheim, California, USA. **AMD-vol 230 and BED-vol 41**: 95–114.

2. Du Bois, P., Chou, C., Fileta, B., Khalil, T., King, A., Mahmood, H., Mertz, H. and Wismans, J. (2004). *Vehicle Crashworthiness and Occupant Protection*, American Iron and Steel Institute, Southfield, MI, USA.

3. Johnson, W. and Mamalis, A.G. (1978). *Crashworthiness of Vehicles*. David Green Printers, Kettering, Great Britain.

4. Jones, N. (1997). *Structural Impact*, Cambridge University Press, Cambridge, UK.

5. Carruthers, J.J., Kettle, A.P. and Robinson, A.M. (1998). Energy Absorption Capability and Crashworthiness of Composite Material Structures: A Review, *Applied Mechanics Reviews*, **51**(10): 635–649.

6. Arnaud, P. and Hamelin, P. (1998). Dynamic Characterization of Structures: A Study of Energy Absorption in Composite Tubes, *Composite Science and Technology*, **58**(5): 709–715.

7. Beard, S.J. and Chang, F.K. (2002). Energy Absorption of Braided Composite Tubes. *International Journal of Crashworthiness*, **7**(2): 191–206.

8. Farley, G.L. (1983). Energy Absorption of Composite Materials, *Journal of Composite Materials*, **17**(5): 267–279.

9. Hamada, H. and Ramakrishna, S. (1996) Comparison of Static and Impact Energy Absorption of Carbon Fiber/Peek Composite Tubes, In: Deo, R.B. and Saff, C.R. (eds), *Composite Materials: Testing and Design*, *ASTM STP 1274*. American Society for Testing and Materials.

10. Mamalis, A.G., Robinson, M., Manolakos, D.E., Demosthenous, G.A., Ioannidis, M.B. and Carruthers, J.J. (1997). Crashworthy Capability of Composite Material Structures: A Review, *Composite Structures*, **37**(2): 109–134.

11. Hull, D. (1991). A Unified Approach to Progressive Crushing of Fibre-reinforced Composite Tubes, *Composites Science and Technology*, **40**: 377–421.

12. Schultz, M.R. and Hyer, M.W. (2001). Static Energy Absorption Capacity of Graphite-epoxy Tubes, *Journal of Composite Materials*, **35**(19): 1747–1761.

13. Coenen, V., Hatrick, M., Law, H., Brosius, D., Nesbitt, A. and Bond, D. (2005). A Feasibility Study of Quickstep Processing of an Aerospace Composite Material, In *SAMPE Europe*, Paris, France, April 5–7, pp. 470–475.

14. Zhang, J. and Fox, B.L. (2005). Manufacturing Process Effects on the Mode I Interlaminar Fracture Toughness and Nanocreep Properties of Cfrp, In: *Proceedings of the 26th International SAMPE Europe Conference*, Paris, April 5–7, pp. 537–543.

15. Li, W. and Miwa, K. (2003). Quick Cure Carbon Fiber Reinforced Epoxy Resin. Patent App. No. 20030082385. Toray Composites (America) Inc. USA.

16. Silcock, M., Garschke, C., Hall, W. and Fox, Bronwyn, L. (2005). A Novel Method of Tube Manufacture for Vehicle Crashworthiness Utilising the Quickstep Process, In: *SAMPE Europe*, Paris, France, April 5–7, pp. 239–244.

17. Kim, Y.N., Im, K.H., Park, J.W. and Yang, J.Y. (2002). An Experimental Study on the Impact Collapse Characteristics of Cf/Epoxy Circular Tubes, In: *Review of Quantitative Nondestructive Evaluation*, Vol. 22, pp. 996–1002, American Institute of Physics, Western Washington University, Bellingham, Washington.

18. Lu, G. and Yu, T. (2003). *Energy Absorption of Structures and Materials*, Woodhead Publishers Limited, Abington Hall, Abington, Cambridge, CB1 6AH, England.

19. Fang, X. and Scola, D.A. (1999). Investigation of Microwave Energy to Cure Carbon Fiber Reinforced Phenylethynyl-terminated Polyimide Composites, Peti-5/Im7. *Journal of Polymer Science: Part A: Polymer Chemistry*, **37**(24): 4616–4628.

20. Ramakrishna, S. and Hamada, H. (1998) Energy Absorption Characteristics of Crashworthy Structural Composite Materials, *Key Engineering Materials*, **141**–**143**: 585–620.